6

CRIPTO and its signaling partner GRP78 drive the metastatic phenotype in human osteotropic prostate cancer

Eugenio Zoni
Lanpeng Chen
Zoraide Granchi
Esther I. Verhoef
Sofia Karkampouna
Federico La Manna
Rob C. M. Pelger
Ewa Snaar-Jagalska
Geert J.L.H. van Leenders
Lijkele Beimers
Peter Kloen
Peter C. Gray
Gabri van der Pluijm
Marianna Kruithof-de Julio

Manuscript Provisionally Accepted

Abstract

Prostate cancer (PCa) is the most prevalent cancer in men and metastatic spread to bone is detected in up to 80% of patients with advanced disease at autopsy. PCa can progress from treatable androgen-dependent stage to castration-resistant stage with distant metastases for which novel therapeutic targets and strategies are urgently needed. Here we identify the cell surface/secreted oncoprotein Cripto as a potential target for the diagnosis and treatment of metastatic PCa. We show that high expression levels of Cripto correlate with poor survival in stratified risk groups of PCa patients and demonstrate that Cripto and its signalling partner Grp78 are highly expressed in PCa metastases. We find that Cripto and Grp78 are expressed at substantially higher levels in the metastatic $ALDH^{high}$ subpopulation of PC-3M-Pro4luc2 PCa cells compared to non-metastatic $ALDH^{low}$. In order to mimic the bone metastatic niche *in vitro,* we cultured the highly osteotropic PC-3M-Pro4luc2 PCa cells with differentiated primary human osteoblasts. This strongly induces Cripto and Grp78 expression in the PCa cells and increases the size of the $ALDH^{high}$ subpopulation relative to the $ALDH^{low}$ in PC-3M-Pro4luc2. Additionally, Cripto or Grp78 knockdown decreases cell proliferation, migration, clonogenicity and the size of the metastasis-initiating $ALDH^{high}$ subpopulation. Significantly, we find that Cripto knockdown reduces the dissemination and invasion of PC-3M-Pro4luc2 cells in a zebrafish model and strongly inhibits bone metastasis in a preclinical mouse model. Taken together, our findings highlight a functional role for Cripto and Grp78 in PCa metastasis and suggest that targeting Cripto/Grp78 signaling may have significant therapeutic potential.

Introduction

Prostate cancer (PCa) is the second most common cancer in men worldwide (1). While current treatments of primary tumors are initially very effective, these beneficial responses are often followed by tumor recurrence and incurable bone metastasis. Therefore, identifying molecular mediators of PCa relapse and metastasis will aid in the development of therapies for this deadly phase of the disease.

Cripto (TDGF1, Cripto-1) is a small, GPI-anchored/secreted foetal-oncoprotein that plays important roles in regulating stem cell differentiation, embryogenesis, tissue growth and remodeling (2). Cripto promotes transformation, migration, invasion and angiogenesis and its misregulation can contribute to cancer development and progression in multiple malignancies, including breast cancer and PCa, which are both characterized by osteotropism in their metastatic stage (3,4). Cripto modulates crucial pathways that regulate bone metastasis such as the TGF-β pathway (5) and functions as an obligatory co-receptor for Nodal, a TGF- β superfamily member that promotes epithelial to mesenchymal transition (EMT) in PCa (5-7). Glucose-regulated protein 78 (Grp78) was identified as a Cripto binding protein and essential mediator of Cripto signaling (8-10). Grp78 is well established as a key survival factor in development and cancer (8,9) and, notably, up-regulation of Grp78 has been associated with the development of castration resistant PCa (CRPC) (11). While Cripto was reported to impact primary human prostate adenocarcinomas (6), its role in driving CRPC and PCa bone metastasis remains unknown.

Here, we investigated the roles of Cripto and Grp78 in aggressive, metastatic human PCa cells both *in vitro* and *in vivo* using an embryonic zebrafish model and a pre-clinical mouse model of experimentally induced PCa bone metastasis. We find that Cripto and Grp78 are upregulated in clinical samples of PCa metastases from human patients and in the highly metastatic $ALDH^{high}$ stem/progenitor-like subpopulation of a human castration resistant PCa cell line (12,13). We further demonstrate that knockdown of Cripto or Grp78 in these cells decreases the size of the stem/progenitor-like subpopulation and also inhibits their extravasation following inoculation into zebrafish and their metastatic potential in a preclinical mouse model of bone metastasis *in vivo*. Together, these findings provide new evidence that Cripto and Grp78 may drive metastatic PCa and highlight the therapeutic potential of targeting the cell surface Cripto/Grp78 complex for the treatment of this deadly disease.

Materials and Methods

PCa Cell lines and culture conditions

Human osteotropic PCa PC-3M-Pro4luc2 cells were maintained in DMEM with 10% FCII, 0.8 mg/ml Neomycin (Santa Cruz, USA) and 1% Penicillin-Streptomycin (Life Technologies, USA). C4-2B cells were maintained in T-medium DMEM (Sigma-Aldrich, The Netherlands) with 20% F-12K nutrient mixture Kaighn's modification (GibcoBRL, USA), 10% FCS, 0.125 mg/ml biotin, 1% Insulin-Transferrin-Selenium, 6.825 ng/ml T3, 12.5 mg/ml adenine and 1% Penicillin/Streptomycin. Primary human osteoblasts were differentiated at confluence: ascorbic acid (50 mg/ml, MERCK, USA) was added in DMEM with 10% FCS, 1% Penicillin-Streptomycin and 1% MEM Non-essential Amino Acids (Gibco-Thermo Scientific, USA). Upon detection of nodules (day 11), medium was supplemented with β-glycerolphosphate (5mM, Sigma, the Netherlands) and 100 nM dexamethasone. After 3 weeks, cells were washed with phosphate buffered saline (PBS) and fixed with 4% paraformaldehyde (PFA). Culture was analyzed for osteogenesis with Alizarin Red staining (ICN Biomedicals, USA) (14). Cells were maintained at 37°C, 5% CO_2

Suppressing Cripto and Grp78 expression with shRNAs

Short hairpin RNAi constructs for Cripto1 (TDGF1 clone# TRCN004889, TRCN004890 and TRCN004891) and HSPA5 (Grp78 clone# TRCN231123, TRCN218611) were obtained from Sigma's MISSION library (Core Facility at LUMC). 500 µL of shRNA-lentiviral vector and 8 µg Polybrene (Sigma, USA) were added to PC-3M-Pro4Luc2 and PC-3M-Pro4Luc2_dTomato cells and incubated for 2 hours. Scrambled shRNA (SHC002, non-targeted, NT or control) with lack of homology for any mammalian mRNA sequence was used as negative control. Cells were selected using puromycin (1µg/ml, Sigma, USA).

Flow Cytometry and aldehyde dehydrogenase assay

PC-3M-Pro4Luc2 were fluorescently labelled with PKH26 Red Fluorescent Cell Linker Kit according to protocol (Sigma-Aldrich, MO, USA). 900.000 cells were seeded in a 10 cm petri dish on a layer of confluent and differentiated human osteoblast. After 48 hours cells were washed with PBS, 1mM EDTA and harvested using trypsin. Fluorescently labelled PC-3M-Pro4Luc2 cells were separated from osteoblast with BD FACS ARIA (BD Biosciences, USA). Non-labelled PC-3M-Pro4Luc2 cells; labelled PC-3M-Pro4Luc2 tumor only and osteoblast only cells were included as controls. Aldehyde dehydrogenase (ALDH) activity was measured using ALDEFLUOR kit (StemCell

Technologies, Durham, USA) (12). Data were analyzed with FCS Express (De Novo software).

Western Blot

Cells were washed with PBS and proteins were extracted with RIPA buffer. Proteins were quantified using Pierce Protein Quantification Assay (ThermoFisher scientific, USA) and 10µg of samples separated by 10% SDS-PAGE and transferred to a blotting membrane using standard techniques. Signal was detected after incubation with 1:1,000 primary antibody (anti-Cripto, #PBL6900, (15)) and with 1:10,000 secondary horseradish peroxidase (HRP) antibody (Promega, USA).

Cripto overexpression

Cripto construct was generated as previously described (16). PC-3M-Pro4Luc2 cells were transfected with Lipofectamine2000 (Life Technologies, USA) and C4-2B cells with Fugene HD (Promega, USA) according to supplier's protocol. Five hours after transfection, the culture medium was replaced. Before collection, cells were washed with PBS and RNA extracted using Trizol (Invitrogen, USA).

RNA isolation and real-time qPCR

After viable cell sorting with ALDEFLUOR Assay Kit (Stem Cell Technologies, USA) (12), total RNA was isolated with Trizol Reagent (Invitrogen, USA) and cDNA synthesized by reverse transcription (Promega, USA) according to protocol. qRT-PCR was performed with BioRad CFX96 (Biorad, The Netherlands). Gene expression was normalized to GAPDH, HPRT and Actin. Primers are listed in Supplementary Table 1.

Proliferation assay

Cells were seeded at density of 1,500 cells/well and allowed to grow for 24, 48, and 72 hours. Proliferation was assessed with 3-(4,5 dimethylthiazol- 2- yl)- 5 -(3 -carboxymethoxyphenyl)- 2 -(4 -sulfophenyl)- 2 H-tetrazolium after 2 hours incubation at 37°C. (CellTiter96 Aqueous assay, Promega, USA). Data were normalized for number of cells.

Transwell migration assay

Migration assays were performed using 24-well transwells (8 mm, Corning Life Sciences, The Netherlands) (13). For the experiments with conditioned medium from osteoblast, this was diluted in the lower chamber 1:2 with medium (50% condition) or administered un-diluted (100% condition).

Colony formation assay

Clonogenic assay was performed in 6 well-plate. 100 cells were seeded in 2mL of medium supplemented with 10% FCII. After 2 weeks, plates were washed with PBS, cells fixed with 4% PFA and colonies stained with 0.1% crystal violet (Sigma-Aldrich, The Netherlands). Plates were imaged before processing the data (17).

Zebrafish maintenance, embryo preparation and tumor cell inoculation

Tg(fli1:GFP)i114 zebrafish line (18,19) was handled and maintained according to local animal welfare regulations to standard protocols (www.ZFIN.org). 2 days-post fertilization (dpf) dechorionized zebrafish embryos were anaesthetized and injected with PC-3M-Pro4Luc2 cells fluorescently labelled as we previously described (13,20). Data are representative of at least two independent and blind experiments with equal or more than 30 embryos per group. Experiments with survival rate of control group lower than 80% were discarded.

Mice

Male 4-5 week-old athymic nude mice (Balb/c *nu/nu* n=10 per group) were purchased from Charles River (L'Arbresle, France). Animals were housed in individual ventilated cages under sterile condition, and sterile food and water provided *ad libitum*. Animal experiment has been approved by the local committee for animal health ethics and research of Leiden University (DEC #14226) and carried out in accordance with the European Communities Council Directive 86/609/EEC.

Intracardiac PCa cell injection and whole body bioluminescent imaging (BLI)

A single cell suspension ($1x10^5$ PC-3M-Pro4Luc2 Cripto knock-down (KD) or non-targeted (NT) control cells per 100 µl PBS) was injected into the left ventricle of anesthetized 5-week old male nude mice (Balb/c nu/nu). Tumor growth and metastasis formation was monitored weekly by bioluminescent reporter imaging (BLI) using IVIS100 Imaging System (Caliper LifeSciences, USA) (12). Analyses of images was performed and quantified with Living Image 4.2 (Caliper Life Sciences, USA).

Immunofluorescence

Immunofluorescence staining was performed on 5-µm paraffin embedded sections. For antigen retrieval, sections were boiled in antigen unmasking solution (Vector Labs, UK) and incubated in 3% H_2O_2 for sequestering endogenous peroxidase (21). Sections were stained with Cripto antibody (#PBL6900, (15)). After blocking with 1% bovine serum albumin (BSA)-PBS-0.1% Tween-20, sections were incubated with primary antibody (1:1000) overnight at 4°C. Detection of Cripto was enhanced using tyramide amplification (Invitrogen/Molecular Probes, USA) and by incubation of slides with horseradish peroxidase (HRP-conjugated secondary antibody (Invitrogen/Molecular Probes, USA), diluted 1:100), followed by incubation with tyramide-488 for 10 minutes (21). Nuclei were visualized by TO-PRO3 (Invitrogen/Molecular Probes, 1:1000 diluted in PBS-0.1% Tween-20) or DAPI. Images were acquired with Leica SP8 confocal (Leica, Germany).

Immunohistochemistry

5 µm formalin fixed, paraffin embedded (FFPE) sections were dewaxed and rehydrated using xylene and ethanol, and endogenous peroxidase was blocked for 20 minutes in 0.3% H_2O_2 in PBS. Heat-induced antigen retrieval was done in TRIS-EDTA buffer (pH=9, 4397-9001, Klinipath, The Netherlands) with a pressure cooker (1.2 bar). Antibodies (anti-Cripto, #PBL6900, 1:1,000 (15); Anti-Cytokeratin 18 (CK18) diluted 1:1,000, Clone DC10, Dako, USA) were diluted 1:1,000 in PBS-BSA 0.1% and incubated overnight at 4°C. Envision (K500711, DAKO, USA) was used to visualize the antibody, followed by counterstaining with hematoxylin.

Human Material

Clinical prostate cancer bone metastasis (10 patients) were collected, stored and issued by the Erasmus MC Tissuebank under ISO 15189:2007 standard operating procedures. Use of these materials for research purposes is regulated according to the Human Tissue and Medical Research: Code of conduct for responsible use (2011). Confirmation that the Medical Research Involving Human Subjects Act (WMO) does not apply to the present study was obtained by the local ethics committee since the research was performed on “waste material” (3 patients) collected from Academisch Medisch Centrum, Amsterdam.

Statistical analysis

Statistical analysis was performed with GraphPad Prism 6.0 (GraphPad software) using t-test or ANOVA for comparison between more groups. Data is presented as mean ± SEM. P-values ≤ 0.05 were considered to be statistically significant (* $P < 0.05$, ** $P < 0.01$, *** $P < 0.001$).

Results

Cripto is highly expressed in metastasis from human PCa patients and correlates with poor survival

Cripto and its signaling partner Grp78 have each been shown to play important roles in primary tumor development and bone metastasis (22). We investigated the correlation of survival with Cripto expression in two independent sets of publically available PCa datasets (GSE21032 and GSE10645 (23,24)). In both datasets Cripto expression was associated with poor prognosis (**Fig. 1 A and B** top; Hazard Ratio (HR)=1.87 and p=0.001 for GSE10645 and HR=2.2 and p=0.06 for GSE21032). Additionally, in both datasets, the expression of Cripto in stratified risk groups was significantly higher in the high vs. low risk group (**Fig. 1 A and B** Bottom; p=1.13e-103 for GSE10645 and p=3.68e-23 for GSE21032). We further investigated the expression of Cripto and Grp78 in the Ramaswamy Multi-cancer dataset from Oncomine™ (Compendia Bioscience), which compares PCa metastasis to primary sites in 76 samples (25) and found that Cripto and Grp78 are significantly upregulated in metastasis compared to primary sites in human PCa (**Fig. 1C**, p=7.15e-4 for Cripto and p=0.03 for Grp78; 1=primary site; 2=metastatic site). Given its expression in metastasis and its correlation with survival, we subsequently investigated the expression of Cripto in PCa bone metastasis by immunostaining of paraffin embedded sections of bone metastasis freshly isolated from patients. We detected significant expression of Cripto and co-localization of Cripto with cytokeratin-18 in serial sections from each of the 13 specimens analyzed (**Fig. 1D**). Moreover, immunostaining with the same antibody revealed that Cripto is also prominently expressed in experimentally induced bone metastasis tissue resulting from intracardiac injection of human castration resistant PC-3M-Pro4Luc2 PCa cells in mice **(Suppl. Fig 1).** Taken together, these data demonstrate that Cripto is selectively expressed in aggressive and metastatic PCa and that its expression correlates with poor prognosis.

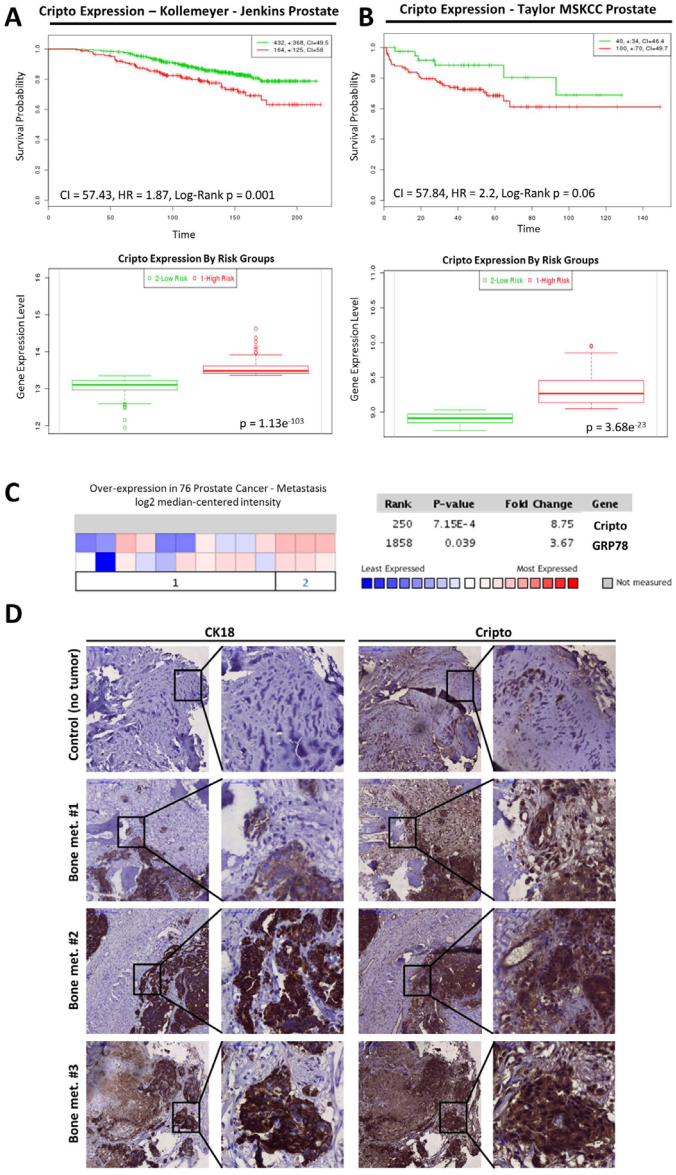

Figure 1. Cripto is expressed in PCa metastasis from human patients and correlates with poor patient prognosis. **A-B**) Top panels: Kaplan-Meier survival curves of censored Cox analysis in Kollemeyer-Jenkins prostate and Taylor-MSKCC prostate database stratified by maximized Cripto expression risk groups. Red = high expression; Green = low expression. Bottom panels: Cripto expression levels stratified by risk groups. Red = high Risk and high Cripto expression; Green = low risk and low Cripto expression **C**) Cripto and Grp78 are significantly up-regulated in PCa metastasis. The Ramaswamy Multi-cancer publicly available dataset (data accessed from www.oncomine.org) was used

for analysis. Colors are Z-score normalized and represent from lower (blue) to higher (red) expression. 1 = primary site; 2 = metastasis. **D**) Representative images of serial sections of PCa bone metastasis stained for CK18 and Cripto and counter stained with hematoxylin (N=13) at lower (10X) and higher (40X, see inserts) magnification.

Co-culture with primary human osteoblasts augments the size of the ALDH^{high} subpopulation, increases Cripto and Grp78 expression levels and promotes the metastatic phenotype of PCa cells

Human PCa cell lines (PC-3M-Pro4Luc2 and C4-2B cells) express detectable levels of Cripto and Grp78 mRNA (**Fig. 2A**). We previously reported that the ALDH^{high} subpopulation of PC-3M-Pro4Luc2 cells displays stem/progenitor-like properties and is highly metastatic relative to their ALDH^{low} counterpart (12). Cripto and Grp78 are expressed in human PCa cell lines (PC-3M-Pro4Luc2 and C4-2B cells) (**Fig. 2A**) and given their known roles in regulating stem cell function and tumor aggressiveness, we tested if Cripto and Grp78 are selectively expressed in the ALDH^{high} subpopulation. Indeed, qRT-PCR analysis on selected subpopulation of cells isolated after viable cell sorting, showed that both Cripto and Grp78 are highly expressed in ALDH^{high} vs. ALDH^{low} subpopulation ($p<0.01$ for Cripto) (**Fig. 2B**). This result is consistent with a role for Cripto and Grp78 in promoting PCa metastasis.

In PCa and other cancers, the osteoblastic microenvironment functions as premetastatic niche by attracting bone-metastasizing tumor cells (26-28). We developed a model of the bone metastatic niche in which primary human osteoblasts are co-cultured with PC-3M-Pro4Luc2 cells *in vitro*. Differentiation of the human osteoblasts was confirmed by Alizarin red staining (**Suppl. Fig 2A**). We find that in the presence of osteoblasts the size of PCa cell ALDH^{high} subpopulation was dramatically increased compared to the size of the ALDH^{high} subpopulation in PCa cells cultured alone (co-culture=60% vs. control=15%, $p<0.05$) **(Fig. 2C)**. Moreover, mRNA analysis after viable cell sorting of fluorescently labelled PC-3M-Pro4Luc2 cells (co-cultured cells compared to control), showed significant increase in Cripto ($p<0.05$) and Grp78 expression **(Fig. 2D)**. In addition, conditioned medium (CM) collected from osteoblasts positively influenced the migratory capability of PC-3M-Pro4Luc2 cells. The increase in migration was directly proportional to the concentration of the conditioned medium used in the experimental setting ($p<0.001$ for 50% CM + 50% not-CM vs. control; $p<0.001$ for 100% CM vs. control and $p<0.001$ for 100% CM vs. 50% CM) **(Fig 2E)**. In line with these observations, administration of osteoblast conditioned medium led to the acquisition of a motile, mesenchymal phenotype in PC-3M-Pro4Luc2 PCa cells as indicated by a decrease in the mRNA expression of the epithelial marker E-Cadherin ($p<0.05$), a

concomitant increase in the mesenchymal markers ZEB1 and ZEB2 ($p<0.05$ for both genes) **(Suppl. Fig. 2B)** and a significant reduction of the ratio E-Cadherin/Vimentin ($p<0.05$) and ratio E-Cadherin/N-Cadherin **(Fig. 2E)**. Together, these data indicate that co-culture with osteoblasts promotes the metastatic phenotype of PCa cells.

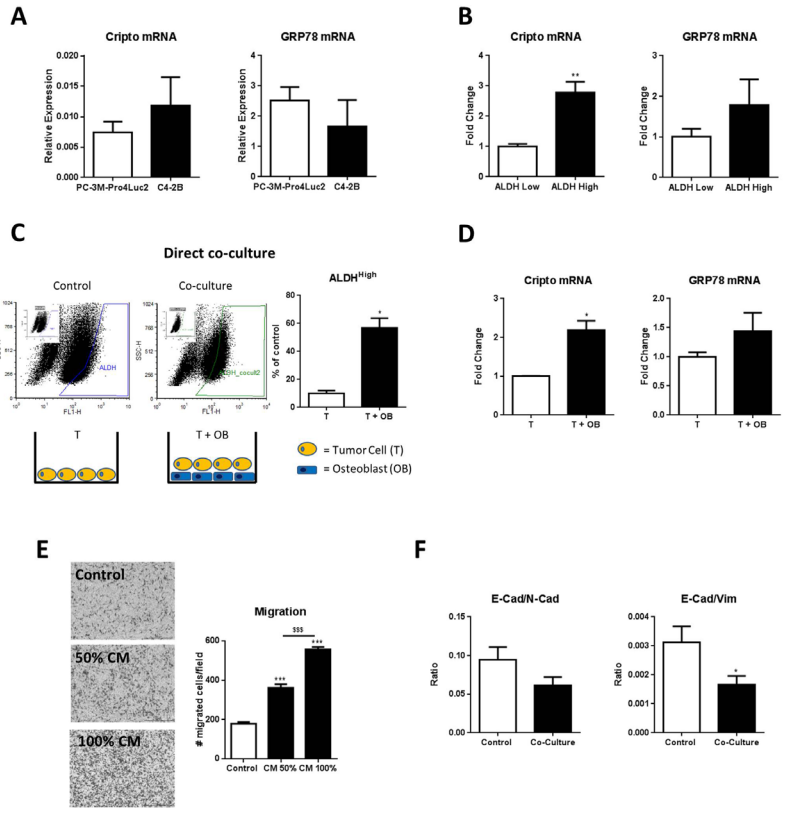

Figure 2. Co-culture with human osteoblasts increases expression of Cripto and Grp78 and cancer stem cell properties of human PCa cells. A) Cripto and Grp78 are expressed in PC-3M-Pro4Luc2 and C4-2B human PCa cell lines. Error bars ± SEM. **B**) Cripto and Grp78 are significantly up-regulated in highly metastatic subpopulation of ALDH^{high} PCa cells vs. low metastatic ALDH^{low} in PC-3M-Pro4Luc2 cells. Error Bars ± SEM **C**) Direct co-culture of fluorescently-labeled PC-3M-Pro4Luc2 human PCa cells (T) with differentiated human osteoblasts (OB) for 48h increases the size of the ALDH^{high} subpopulation in PCa cells. Error Bars ± SEM. **D**) mRNA analysis shows increased Cripto and Grp78 expression after co-culture. Error Bars ± SEM. **E**) Conditioned medium (CM) from human osteoblast enhances migration of PC-3M-Pro4Luc2 human PCa cells. Error Bars ± SEM. **F**) Co-culture of PC-3M-Pro4Luc2_dTomato PCa cells for 48h with human osteoblast induces a shift to mesenchymal phenotype as indicated by significant decrease in ratio E-Cad/Vim and E-Cad/N-Cad. Error Bars ± SEM. *, P<0,05; **, P<0,01; *** and $$$, P<0,001.

Cripto and Grp78 maintain stem cell-like properties of aggressive human PCa cells *in vitro*

In order to test the function of Cripto and Grp78 in human PCa cells, we generated stable knockdown lines in PC-3M-Pro4Luc2 and C4-2B cells and validated reduced expression of Cripto and Grp78 by Western Blot and qRT-PCR **(Fig. 3A, Suppl. Fig 3A and Suppl. Fig. 4A)**. As previously shown by others in PC3 cells and consistent with the extensive post-translational modification of Cripto, we detected two protein bands of approximately 17 and 25 kDa (5,29) **(Fig. 3A)**. Cripto knockdown lines (shRNA#2 and #3) both show decreased cell proliferation ($p<0.001$ at 24h for shRNA#2 and $p<0.001$ at 24, 45, 72h for shRNA#2 and shRNA#3) **(Fig. 3B).** No effect on cell proliferation was observed in the C4-2B Cripto knockdown cells **(Suppl. Fig. 3B).** The PC-3M-Pro4Luc2 Cripto knockdown cells also had a significantly reduced percentage of metastatic, stem cell-like $ALDH^{high}$ cells relative to non-targeted control cells ($p<0.05$ for shRNA#2 and p=ns for shRNA#3) **(Fig. 3C)**. Grp78 knockdown similarly displayed reduction of the size of $ALDH^{high}$ subpopulation of cells ($p<0.05$ for shRNA#1 and p=ns for shRNA#2) **(Suppl. Fig. 4B)**.

We previously reported that the $ALDH^{high}$ subpopulation of PC-3M-Pro4Luc2 is enriched for cells with increased clonogenicity and migratory properties relative to the $ALDH^{low}$ cell subpopulation (12). Here we show that PC-3M-Pro4Luc2 Cripto knockdown cells have significantly reduced clonogenicity relative to control cells as measured by the number and area of colonies produced ($p<0.05$) **(Fig. 3D)**. This effect appeared to be specific since transfection of a non-targetable Cripto expression construct resulted in significant rescue of the loss of clonogenicity caused by the Cripto shRNA ($p<0.001$ for colony number and $p<0.05$ for colony area) **(Fig. 3D).** Grp78 knockdown in PC-3M-Pro4Luc2 human PCa cells also resulted in a decrease in the number of colonies ($p<0.05$) and a similar trend was shown for colony area **(Suppl. Fig 4C)**. Finally, Cripto knockdown significantly reduced the migratory capability of both cell lines ($p<0.05$ and $p<0.01$ respectively, **Fig. 4A and B**). Complete (PC-3M-Pro4Luc2) or partial (C4-2B) rescue of the effects of shRNA knockdown could be again achieved by the non-targetable Cripto expression construct **(Fig. 4C and D)**. Grp78 knockdown in PC-3M-Pro4Luc2 cells also resulted in a significant reduction of migratory potential ($p<0.001$ for both shRNAs) (Suppl. Fig. 4D). Together, these data suggest that Cripto and Grp78 are required to maintain the stem cell-like phenotype of PC-3M-Pro4Luc2 cells.

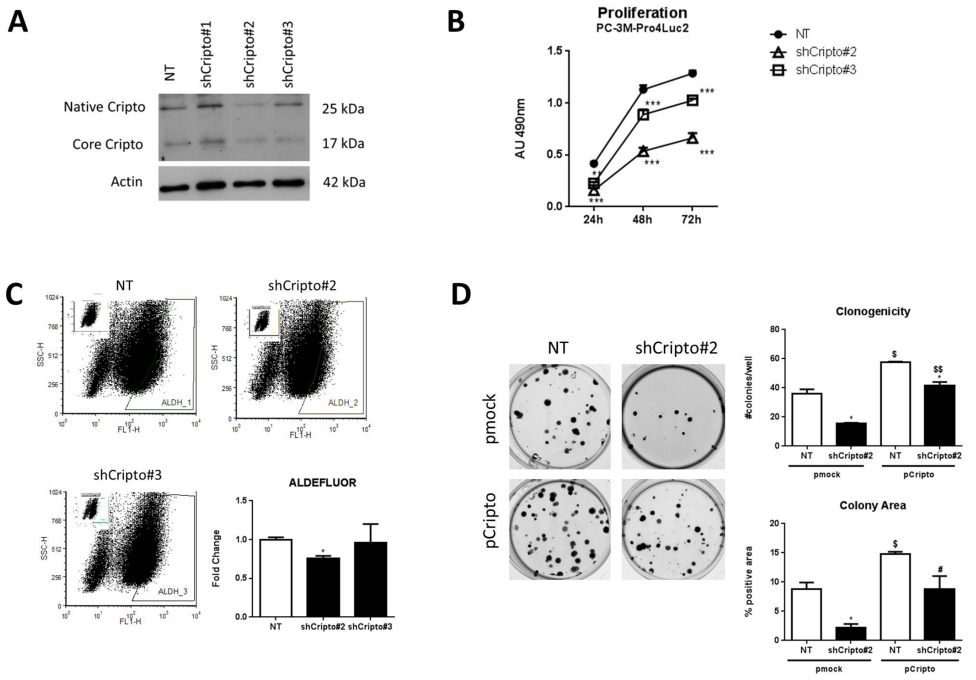

Figure 3. Cripto knock-down causes loss of the stem cell-like phenotype in PCa cells. **A**) Western Blot analysis of Cripto expression in control (scrambled shRNA, NT) PC-3M-Pro4Luc2 (first lane) and Cripto knock-down PC-3M-Pro4Luc2 cells with shCripto#1, #2, #3, derived from different shRNA constructs. Two bands of respectively 25 KDa (Native) and 17 KDa (Core) for Cripto are detected as previously shown (see Results). **B**) Knockdown of Cripto affects the proliferation in PC-3M-Pro4Luc2 . Error Bars ± SEM. **C**) Cripto knock-down leads to a decrease in the size of $ALDH^{high}$ subpopulation in PC-3M-Pro4Luc2 cells. Error Bars ± SEM. **D**) Cripto knockdown affects clonogenic ability and Cripto overexpression is capable of reversing this phenotype in PC-3M-Pro4Luc2. Error Bars ± SEM. * and $ and #, P<0,05; ** and $$, P<0,01; ***, P<0,001.

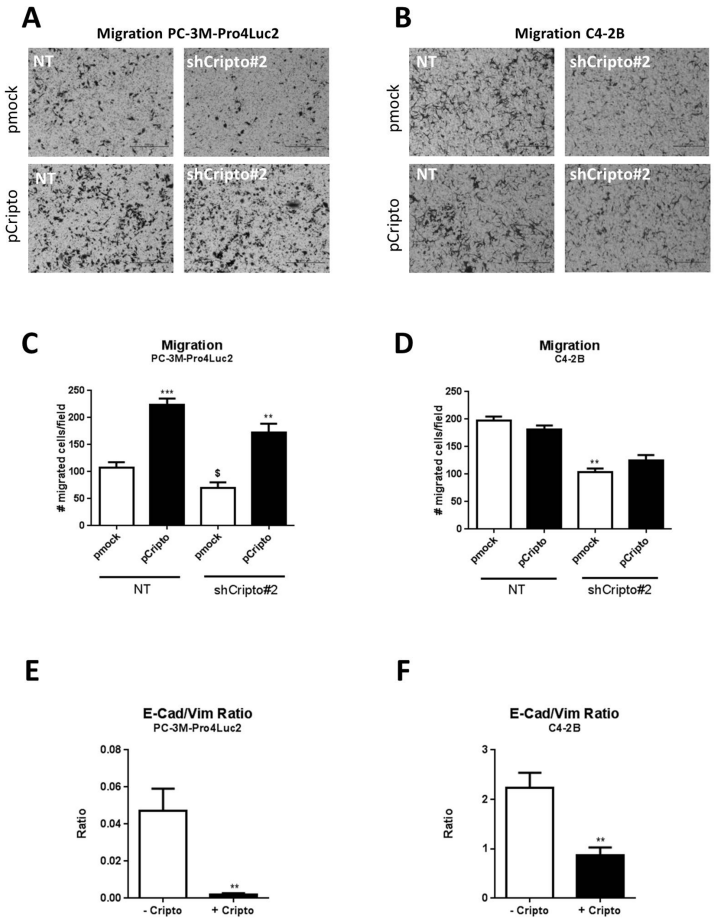

Figure 4. Cripto overexpression promotes PCa cell migration and rescues the Cripto knock-down phenotype. A-B) Cripto Knock-down significantly reduces cell migration in PC-3M-Pro4Luc2 and C4-2B cells and Cripto overexpression (**C-D**) is capable of rescuing completely (PC-3M-Pro4Luc2) or partially (C4-2B) the phenotype. Error Bars ± SEM. **E**) mRNA analysis in PC-3M-Pro4Luc2 cells and C4-2B (**F**) after 48h of Cripto overexpression shows decrease in E-Cad/Vim ratio supporting the switch towards a more mesenchymal phenotype. Error Bars ± SEM. $, P<0,05; **, P<0,01; ***, P<0,001.

Cripto promotes EMT and invasiveness of human PCa cells

EMT is strongly associated with tumor cell invasion and Cripto was recently reported to promote EMT in human PCa (6). Consistent with this study, we found that Cripto overexpression in PC-3M-Pro4Luc2 and C4-2B cells **(Suppl. 5A and B)** causes a strong and significant down-regulation of the epithelial marker E-Cadherin ($p<0.05$) at the mRNA level in both cell lines and an increase in the mesenchymal markers Vimentin, SNAIL2 and TWIST in PC-3M-Pro4Luc2 cells ($p<0.05$, $p<0.05$ and $p<0.01$ respectively) and ZEB1 in C4-2B cells **(Suppl. Fig 5C and D).** Cripto overexpression caused a strong and significant decrease in the ratio of E-Cadherin/Vimentin ($p<0.01$) in both PCa cell lines **(Fig. 4E and F)**. Together, these data support a role for Cripto in promoting EMT and the invasive phenotype in PC-3M-Pro4Luc2 and C4-2B cells.

We have previously shown that zebrafish can be used to effectively evaluate migration and invasion of human PCa cells and the interaction between PCa cells and the vasculature at the single cell level *in vivo* (13,30). Clear detection of extravasating tumor cells in this system is facilitated by the fact that the vascular system of zebrafish embryos is completely functional and the embryos are transparent (31). We tested the role of Cripto and Grp78 in PCa cell extravasation and metastasis by injecting fluorescently-labeled PC-3M-Pro4Luc2 cells with Cripto or Grp78 knocked down into the circulatory system of zebrafish embryos (13). In the first hours disseminated cells arrested in the host vasculature and then we observed extravasation from 12 hpi (hours post implantation) and perivascular tumor cells in multiple foci including the intersegmental vessels, the optic veins, the dorsal aorta and the caudal vein. The perivascular tumor cells invaded the neighboring tail fin exclusively at the posterior ventral end of the caudal hematopoietic tissue (CHT). At day 4 post-implantation (4 dpi), Cripto knockdown caused a significant reduction in extravasation and metastatic tumor growth compared to control cells with scrambled shRNA **(Fig. 5A, B and C)**. Similarly, Grp78 knockdown cells displayed a significant reduction in the tumor growth into the tail fin after invasion from CHT compared to control cells (**Suppl. Fig. 6A and B**). However, invasion was not significantly different in Grp78 knockdown cells compared to control **(Suppl. Fig. 6C)**. Taken together, these data support our *in vitro* findings and reinforce the hypothesis that Cripto/Grp78 signaling plays an important role in the maintenance of an invasive and aggressive phenotype in human PCa.

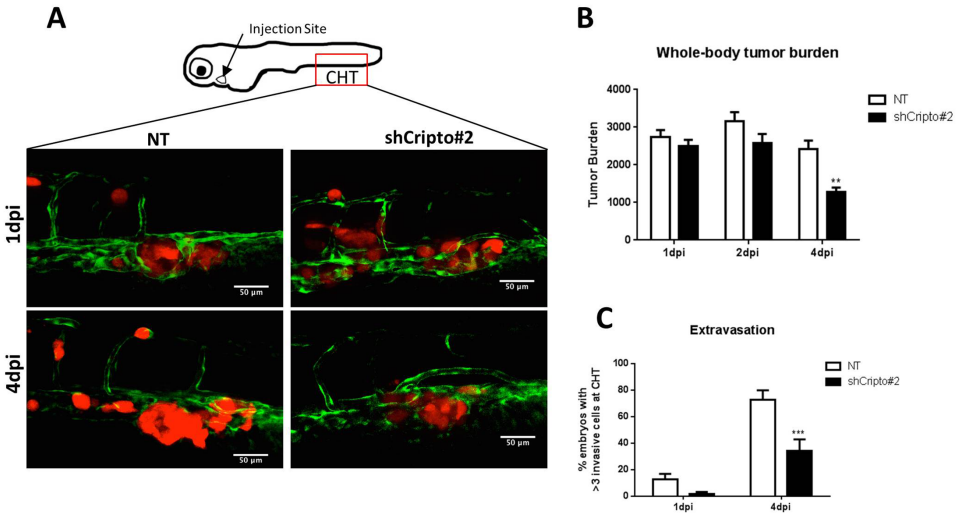

Figure 5. Cripto knockdown reduces invasion and tumor growth of human PCa cells *in vivo*. A) PC-3M-Pro4Luc2_dTomato human PCa cells with scrambled shRNA control (NT) and ShCripto#2 shRNAs have been injected in the duct of Cuvier to monitor extravasation and formation of distant metastasis in vivo. 30 embryos injected/group. **B**) Cripto knock-down reduces whole-body tumor burden at 4dpi (days post injection). Error Bars ± SEM. **C**) Cripto knock-down reduces number of extravasated cells at 1 and 4dpi at the caudal hematopoietic tissue (CHT). Error Bars ± SEM. **, P<0,01; *** P<0,001.

Cripto knockdown decreases metastasis formation *in vivo*

We previously demonstrated that intracardiac injection of luciferase-expressing PC-3M-Pro4Luc2 cells in mice results in bone metastasis (12). Here we used this preclinical mouse model to test the role of Cripto in mediating the metastatic activity of these PCa cells. Cripto knockdown cells or control cells with a scrambled shRNA were injected into the left cardiac ventricle of nude mice (Balb/c nu/nu) and bioluminescence, which reflects tumor size, was measured weekly for the course of the experiment. Quantification of bioluminescent images showed significant reduction in metastasis formation and the number of metastasis in mice inoculated with Cripto knockdown cells compared to mice injected with control cells (week 5, $p<0.05$) **(Fig. 6 A, B, C)**. This result is consistent with the other findings outlined above and suggests that Cripto is required for bone metastasis in a mouse model of human PCa.

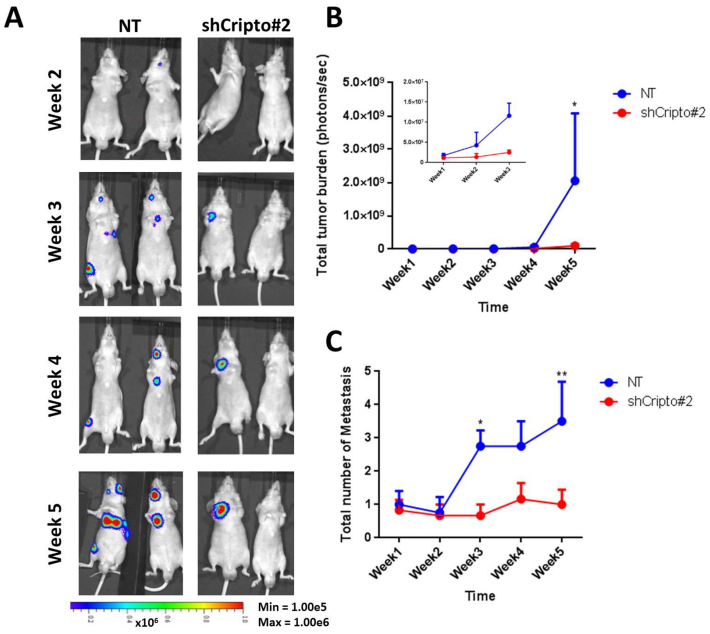

Figure 6. Cripto knockdown inhibits bone metastasis of human PCa cells *in vivo*. **A**) PC-3M-Pro4Luc2 human PCa cells with Cripto knock-down (ShCripto#2) and shRNA scrambled control (NT) have been injected in the left ventricle of nude mice. Formation of distant metastasis was monitored weekly with BLI measurements. Images are representative of 6 animals for Cripto Knock-down and 4 animals for non-targeted control. **B**) Quantification of BLI measurements. Difference is significant at week 5 ($p<0.05$ with two way ANOVA). Cripto knockdown is represented in red, non-targeted control is represented in blue. Error Bars ± SEM. **C**) Total number of metastasis per mouse in mice injected with either Cripto knock-down (ShCripto#2, red) or control (NT, blue) PC-3M-Pro4Luc2 cells, (*, $p<0.05$; **$p<0,01$; with two way ANOVA). Error Bars ± SEM.

Discussion

This study presents evidence supporting a role for Cripto and Grp78 in the regulation of the invasive program of PCa cells that maintains stem cell-like and aggressive phenotypes in human PCa. Cripto/Grp78 signaling is known to regulate stem cells and tumor cells (32) and our results suggest that this signaling may promote the acquisition of a metastatic phenotype in PCa. This phenotype includes the ability of PCa cells to invade the supportive stroma and neighboring tissues to allow subsequent formation of bone metastasis at distant sites (33). Cripto/Grp78 signaling may also play a specific role in metastasis by facilitating initial colonization of the bone by PCa cells.

Our demonstration that Cripto is strongly upregulated in high-risk patient groups compared to low risk groups and that it correlates with poor survival highlight the significance of these proteins in metastatic PCa. Importantly, the selective expression of Cripto and Grp78 in PCa metastasis was substantiated by analysis of publicly available datasets (25) and reinforced by our analysis on 13 samples of PCa bone metastasis derived from CRPC patients.

The $ALDH^{high}$ subpopulation of PC-3M-Pro4Luc2 cells is enriched for tumor initiating cells with metastatic potential and generally accounts for a small percentage of all tumor cells (12,13). Here we show that these highly metastatic $ALDH^{high}$ cells have higher levels of Cripto and Grp78 expression compared to non-stem cell-like, non-metastatic $ALDH^{low}$ cells. This finding supports our hypothesis that Cripto and its cell surface signaling partner Grp78 are restricted to a small subpopulation of cells characterized by high metastatic ability, similar to what was recently shown in breast cancer (15). Our results also support the notion that Cripto signaling promotes EMT (6,7) and the migratory and invasive phenotype in PCa cells associated with a switch from a sessile, epithelial state to a motile, mesenchymal phenotype. Indeed, transcriptional analysis following Cripto overexpression reveals the emergence of an “EMT signature” characterized by a marked reduction in the expression of the epithelial marker E-Cadherin paralleled by a significant increase in the expression of the mesenchymal markers Vimentin, Snail2 and Twist, again indicating the acquisition of the mesenchymal phenotype.

The activation of the bone stroma by metastatic cells alters the physiological balance between osteoblast-mediated bone formation and osteoclast-mediated bone resorption during bone metastatic colonization (34). Strikingly, we found that co-culture of PCa cells with human osteoblasts, important cellular constituents of the bone metastatic niche (34), induced a significant increase in Cripto and Grp78 mRNA

expression in the tumor cells. Osteoblasts have previously been reported to promote the aggressiveness of osteolytic human PCa cells *in vitro* (26). These findings, are in line with our data showing that osteoblasts promote the metastatic phenotype of PCa cells by causing expansion of the ALDH^{high} subpopulation, increasing tumor cell migration and inducing expression of Cripto and Grp78. In light of previous studies demonstrating that Cripto binds cell surface Grp78 and that this interaction is required for Cripto signaling, our results suggest that Cripto and Grp78 function cooperatively to regulate the interaction between tumor cells and osteoblasts within the bone microenvironment. However, given the complexity of the bone metastatic niche, we focused primarily on the role of Cripto and Grp78 in the maintenance of an aggressive and metastatic phenotype in PCa cells. Additional experiments are required to elucidate the interactions between PCa cells and the different components of the bone microenvironment in mechanistic detail.

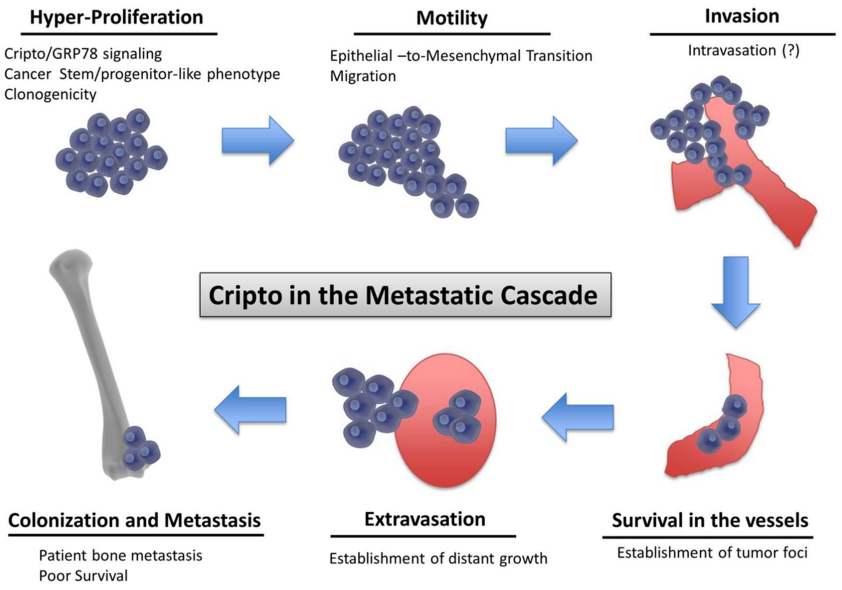

Figure 7. Schematic representation of the proposed role of Cripto in the metastatic cascade in human prostate cancer. Cripto and Grp78 influence cell proliferation and are highly expressed in a subpopulation of highly metastatic stem/progenitor-like cells (ALDH^{high}). Cripto and Grp78 knock-down impairs cell migration, suggesting a role of these genes in the acquisition of an invasive phenotype. Cripto- and Grp78-expressing cells are better adapted to surviving in the circulation and of forming distant metastases in zebrafish and mouse xenograft models.

In conclusion, we demonstrate that Cripto and it signalling mediator Grp78 may play pivotal, functional roles in the acquisition and maintenance of an invasive, metastatic phenotype in human prostate cancer (see schematic representation in **Fig. 7**). Therefore, from a therapeutic and diagnostic point of view, Cripto and Grp78 represent compelling molecules for targeting and monitoring of highly aggressive stem/progenitor-like prostate cancer cells in advanced human prostate cancer.

Acknowledgements

We would like to thank Sofia Karkampouna, Federico La Manna, Janine Melsen and Tim Rodenburg (Dept. of Urology, LUMC, The Netherlands) for discussion about this work and help. We thank Boudewijn Kruithof (Dept. of Molecular Cell Biology, LUMC, the Netherlands) for help and support during the acquisition of high-resolution images. We thank Guido de Roo from the Flow cytometry facility (Dept. of Hematology, LUMC, The Netherlands) for technical support and Jan Kroon (Dept. of Urology, LUMC, The Netherlands) for providing samples of experimental metastasis. We also would like to thank Chris van der Bent and Hetty Sips (Dept. of Endocrinology, LUMC, The Netherlands) for help and technical support.

Grant Support

The research leading to these results has received funding from the FP7 Marie Curie ITN under grant agreement n°264817 - BONE-NET (GP, EZ, ZG). This project receives also additional support from the Dutch Cancer Society under grant agreement UL2015-7599 KWF (MK, GP, PK) and UL2014-7058 - PROPER (GP, LC, ESJ), from Leiden University Fond (MK) and Clayton Foundation (PG). The authors disclose no potential conflicts of interest.

REFERENCES

1. Jemal A, Center MM, DeSantis C, Ward EM. Global patterns of cancer incidence and mortality rates and trends. Cancer Epidemiol Biomarkers Prev 2010;19(8):1893-907.
2. Klauzinska M, Castro NP, Rangel MC, Spike BT, Gray PC, Bertolette D, et al. The multifaceted role of the embryonic gene Cripto-1 in cancer, stem cells and epithelial-mesenchymal transition. Semin Cancer Biol 2014;29:51-8.
3. de Castro NP, Rangel MC, Nagaoka T, Salomon DS, Bianco C. Cripto-1: an embryonic gene that promotes tumorigenesis. Future Oncol 2010;6(7):1127-42.
4. Castro NP, Fedorova-Abrams ND, Merchant AS, Rangel MC, Nagaoka T, Karasawa H, et al. Cripto-1 as a novel therapeutic target for triple negative breast cancer. Oncotarget 2015;6(14):11910-29.
5. Lawrence MG, Margaryan NV, Loessner D, Collins A, Kerr KM, Turner M, et al. Reactivation of embryonic nodal signaling is associated with tumor progression and promotes the growth of prostate cancer cells. Prostate 2011;71(11):1198-209.
6. Terry S, El-Sayed IY, Destouches D, Maille P, Nicolaiew N, Ploussard G, et al. Cripto overexpression promotes mesenchymal differentiation in prostate carcinoma cells through parallel regulation of AKT and FGFR activities. Oncotarget 2014.
7. Pilli VS, Gupta K, Kotha BP, Aradhyam GK. Snail-mediated Cripto-1 repression regulates the cell cycle and epithelial-mesenchymal transition-related gene expression. FEBS Lett 2015;589(11):1249-56.
8. Shani G, Fischer WH, Justice NJ, Kelber JA, Vale W, Gray PC. Grp78 and Cripto form a complex at the cell surface and collaborate to inhibit transforming growth factor beta signaling and enhance cell growth. Mol Cell Biol 2008;28(2):666-77.
9. Lee AS. Grp78 induction in cancer: therapeutic and prognostic implications. Cancer Res 2007;67(8):3496-9.
10. Kelber JA, Panopoulos AD, Shani G, Booker EC, Belmonte JC, Vale WW, et al. Blockade of Cripto binding to cell surface Grp78 inhibits oncogenic Cripto signaling via MAPK/PI3K and Smad2/3 pathways. Oncogene 2009;28(24):2324-36.
11. Pootrakul L, Datar RH, Shi SR, Cai J, Hawes D, Groshen SG, et al. Expression of stress response protein Grp78 is associated with the development of castration-resistant prostate cancer. Clin Cancer Res 2006;12(20 Pt 1):5987-93.
12. van den Hoogen C, van der Horst G, Cheung H, Buijs JT, Lippitt JM, Guzman-Ramirez N, et al. High aldehyde dehydrogenase activity identifies tumor-initiating and metastasis-initiating cells in human prostate cancer. Cancer Res 2010;70(12):5163-73.
13. Zoni E, van der Horst G, van de Merbel AF, Chen L, Rane JK, Pelger RC, et al. miR-25 Modulates Invasiveness and Dissemination of Human Prostate Cancer Cells via Regulation of alphav- and alpha6-Integrin Expression. Cancer Res 2015;75(11):2326-36.
14. van der Horst G, Farih-Sips H, Lowik CW, Karperien M. Hedgehog stimulates only osteoblastic differentiation of undifferentiated KS483 cells. Bone 2003;33(6):899-910.
15. Spike BT, Kelber JA, Booker E, Kalathur M, Rodewald R, Lipianskaya J, et al. Cripto/Grp78 signaling maintains fetal and adult mammary stem cells ex vivo. Stem Cell Reports 2014;2(4):427-39.
16. Gray PC, Shani G, Aung K, Kelber J, Vale W. Cripto binds transforming growth factor beta (TGF-beta) and inhibits TGF-beta signaling. Mol Cell Biol 2006;26(24):9268-78.
17. Guzman C, Bagga M, Kaur A, Westermarck J, Abankwa D. ColonyArea: an ImageJ plugin to automatically quantify colony formation in clonogenic assays. PLoS One 2014;9(3):e92444.
18. Stoletov K, Montel V, Lester RD, Gonias SL, Klemke R. High-resolution imaging of the dynamic tumor cell vascular interface in transparent zebrafish. Proc Natl Acad Sci U S A 2007;104(44):17406-11.

19. Lawson ND, Weinstein BM. In vivo imaging of embryonic vascular development using transgenic zebrafish. Dev Biol 2002;248(2):307-18.
20. He S, Lamers GE, Beenakker JW, Cui C, Ghotra VP, Danen EH, et al. Neutrophil-mediated experimental metastasis is enhanced by VEGFR inhibition in a zebrafish xenograft model. J Pathol 2012;227(4):431-45.
21. Karkampouna S, Kruithof BP, Kloen P, Obdeijn MC, van der Laan AM, Tanke HJ, et al. Novel Ex Vivo Culture Method for the Study of Dupuytren's Disease: Effects of TGFbeta Type 1 Receptor Modulation by Antisense Oligonucleotides. Mol Ther Nucleic Acids 2014;3:e142.
22. Bianco C, Strizzi L, Normanno N, Khan N, Salomon DS. Cripto-1: an oncofetal gene with many faces. Curr Top Dev Biol 2005;67:85-133.
23. Taylor BS, Schultz N, Hieronymus H, Gopalan A, Xiao Y, Carver BS, et al. Integrative genomic profiling of human prostate cancer. Cancer Cell 2010;18(1):11-22.
24. Nakagawa T, Kollmeyer TM, Morlan BW, Anderson SK, Bergstralh EJ, Davis BJ, et al. A tissue biomarker panel predicting systemic progression after PSA recurrence post-definitive prostate cancer therapy. PLoS One 2008;3(5):e2318.
25. Ramaswamy S, Ross KN, Lander ES, Golub TR. A molecular signature of metastasis in primary solid tumors. Nat Genet 2003;33(1):49-54.
26. Morhayim J, van de Peppel J, Demmers JA, Kocer G, Nigg AL, van Driel M, et al. Proteomic signatures of extracellular vesicles secreted by nonmineralizing and mineralizing human osteoblasts and stimulation of tumor cell growth. FASEB J 2015;29(1):274-85.
27. Coleman RE. Clinical features of metastatic bone disease and risk of skeletal morbidity. Clin Cancer Res 2006;12(20 Pt 2):6243s-49s.
28. Shiozawa Y, Pedersen EA, Havens AM, Jung Y, Mishra A, Joseph J, et al. Human prostate cancer metastases target the hematopoietic stem cell niche to establish footholds in mouse bone marrow. J Clin Invest 2011;121(4):1298-312.
29. Saloman DS, Bianco C, Ebert AD, Khan NI, De Santis M, Normanno N, et al. The EGF-CFC family: novel epidermal growth factor-related proteins in development and cancer. Endocr Relat Cancer 2000;7(4):199-226.
30. Ghotra VP, He S, van der Horst G, Nijhoff S, de Bont H, Lekkerkerker A, et al. SYK is a candidate kinase target for the treatment of advanced prostate cancer. Cancer Res 2015;75(1):230-40.
31. Isogai S, Lawson ND, Torrealday S, Horiguchi M, Weinstein BM. Angiogenic network formation in the developing vertebrate trunk. Development 2003;130(21):5281-90.
32. Gray PC, Vale W. Cripto/Grp78 modulation of the TGF-beta pathway in development and oncogenesis. FEBS Lett 2012;586(14):1836-45.
33. van der Pluijm G. Epithelial plasticity, cancer stem cells and bone metastasis formation. Bone 2011;48(1):37-43.
34. Ozdemir BC, Hensel J, Secondini C, Wetterwald A, Schwaninger R, Fleischmann A, et al. The molecular signature of the stroma response in prostate cancer-induced osteoblastic bone metastasis highlights expansion of hematopoietic and prostate epithelial stem cell niches. PLoS One 2014;9(12):e114530.

SUPPLEMENTARY DATA

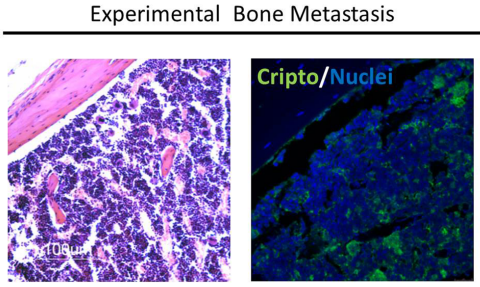

Suppl. Fig 1. Cripto expression in experimental bone metastasis. Cripto expression in experimental bone metastasis derived from intra cardiac inoculation of PC-3M-Pro4Luc2 human PCa cells in a preclinical mouse model of PCa bone metastasis.

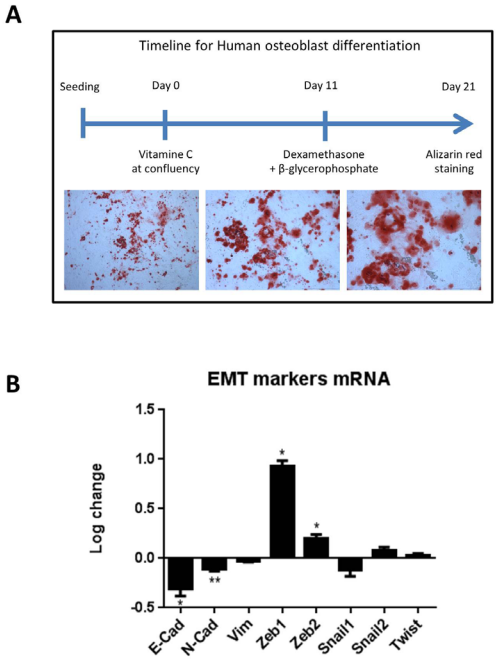

Suppl. Fig 2. Osteoblast differentiation and influence of direct co-culture of tumor cells with human osteoblast on EMT markers. A) Alizarin Red staining of differentiated osteoblast shows efficacy of the differentiation process (see materials and methods). **B**) Co-culture of PC-3M-Pro4Luc2 tumor cells with differentiated primary human osteoblast induces downregulation of E-Cad and strong upregulation of Zeb1 in PC-3M-Pro4Luc2 cells. Error Bars ± SEM. *, P<0,05; **, P<0,01.

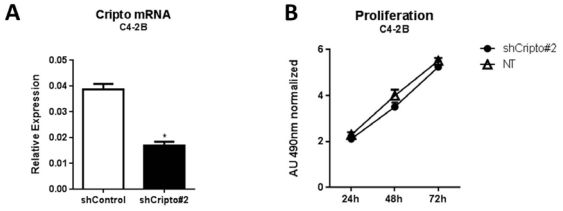

Suppl. Fig. 3. Cripto knock-down in C4-2B cells. A) C4-2B with Cripto knock-down show significanly lower Cripto expression compared to control cells. **B**) Cripto Knock-down does not affect C4-2B proliferation. Error Bars ± SEM. *, P<0,05.

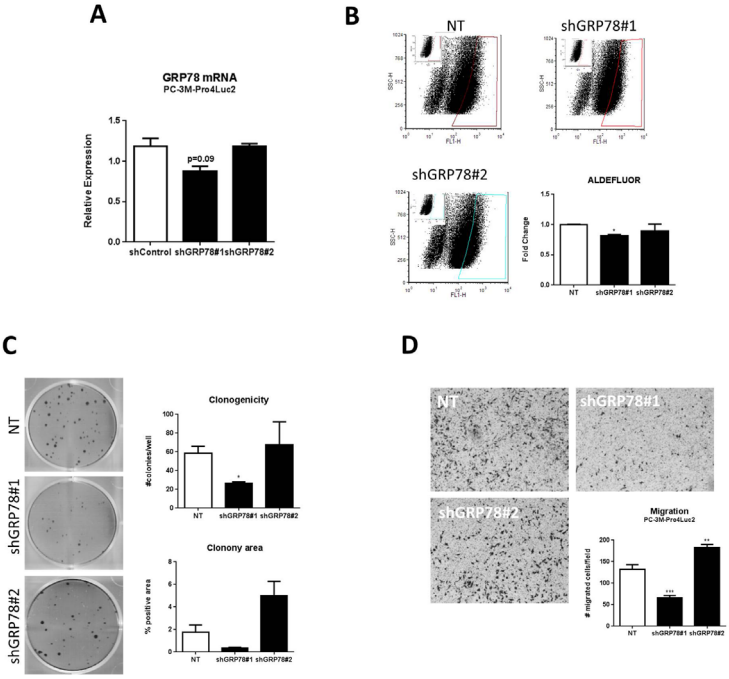

Suppl. Fig. 4. Grp78 Knock-down, functional study. **A**) PC-3M-Pro4Luc2 cells with Grp78 knock-down by two different shRNAs. Error Bars ± SEM. **B**) Grp78 KD reduces the size of ALDHhigh subpopulation of cells in PC-3M-Pro4Luc2 human prostate cancer cells. Error Bars ± SEM. **C-D**) Grp78 KD significanlty reduces clonogenicity and migration of PC-3M-Pro4Luc2 human prostate cancer cells. Error Bars ± SEM. *, P<0,05; **, P<0,01; ***, P<0,001.

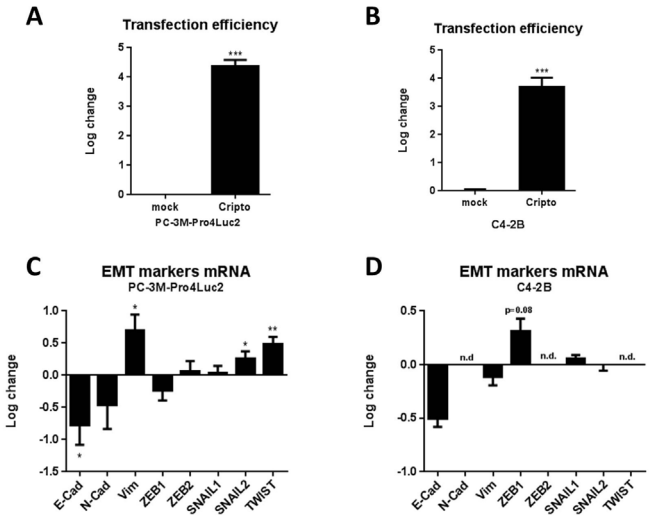

Suppl. Fig. 5. Cripto overexpression in two human prostate cancer cell lines. **A-B**) Tumor cells overexpressing Cripto show significanlty higher Cripto expression compared to mock transfected cells (control). Error Bars ± SEM. **C-D**) Cripto overexpresssion in PC-3M-Pro4Luc2 and C4-B cells induces significant decrease of E-Cad and upregulation of Vim in PC-3M-Pro4Luc2 cells. Error Bars ± SEM. *, P<0,05; **, P<0,01; ***, P<0,001.

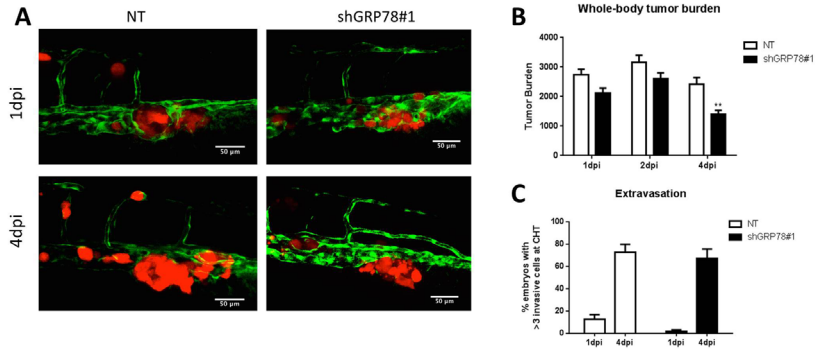

Suppl. Fig. 6. Grp78 KD reduces invasion and tumor growth *in vivo*. A) PC-3M-Pro4Luc2_dTomato human prostate cancer cells with Grp78 knock-down have been injected in the duct of Cuvier to monitor extravasation and formation of distant metastasis in vivo. 30 embryos injected per group. **B-C**) Grp78KD reduces extravasation and tumor growth significantly at 4dpi (days post injection) at the caudal hematopoietic tissue (CHT). No effect on tumor burden is observed. Error Bars ± SEM. (Blind observations). **, P<0,01.

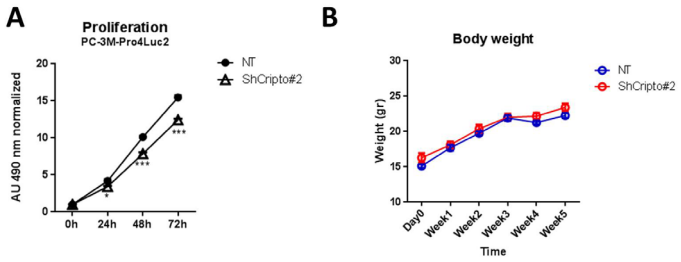

Suppl. Fig. 7. Cripto Knock-down effect on proliferation and measurment of weight of animal injected with matching cells *in vivo*. A) MTS performed on PC-3M-Pro4Luc2 cells with Cripto KD and NT control to confirm KD effect on proliferation prior to inoculation in animals. Experiment performed on same cells injected in vivo. Error Bars ± SEM. **B**) Body weight of animals (shCripto = 6 animals, NT = 4 animals). Error Bars ± SEM. *, P<0,05; ***, P<0,001.